

# Research on the Distribution Law of Wind Speed across Coal Mine Tunnel Cross-Section

Rui Sun

<sup>1</sup>State Key Laboratory of Coal Mine Disaster Prevention and Control, Chongqing 400037, China;

<sup>2</sup> China Coal Technology and Engineering Group Chongqing Research Institute, Chongqing 400037, China

## Abstract

In response to the challenge that the accuracy of wind speed monitoring in tunnels often fails to meet decision - making requirements, the distribution law of wind speed in the cross - sections of rectangular and semi - circular arched tunnels was selected as the research subject. By employing a combined approach of theoretical analysis and numerical simulation, a systematic study was conducted on the wind speed distribution law in the cross - sections of tunnels under various conditions. The research findings reveal that the position of the average wind speed line within the roadway is solely determined by the roadway's dimensions and is independent of other major controlling factors. Specifically, the distance between the average wind speed line and the two sides (top and bottom) of the roadway is approximately 0.11 times the width (height) of the roadway. Numerical simulation results illustrate the wind speed distribution patterns in different types of tunnel cross - sections under diverse conditions. It is observed that the ratio of the maximum wind speed to the average wind speed in tunnel cross - sections is around 1.2. For a semi - circular arch roadway, the distance between the average wind speed line and the roof ranges from 10.76% to 11.12% of the roadway height. In contrast, for a rectangular roadway, this distance ranges from 10.76% to 11.03% of the roadway height, with an error margin of less than 4% when compared to the theoretical calculation results.

## Keywords

Mine ventilation, Wind speed, Tunnel cross-section, Distribution law, Numerical simulation.

## 1. Introduction

The intelligent transformation of coal mines represents an indispensable avenue for the modernization and sustainable development of the coal industry. As coal mining steps into a new epoch characterized by safety and intelligence, the in - depth fusion of intelligent technologies with the coal sector is bound to trigger revolutionary shifts in coal production paradigms, thereby fostering substantial enhancements in both production efficiency and safety standards within coal mines [1]. Mine ventilation intelligent technology plays a pivotal role in mine intelligent construction. It enables real - time monitoring of underground ventilation parameters, ensuring a timely and demand - driven air supply across different time periods and locations [2-4]. This technology is an integral and crucial part of building intelligent mines. Currently, the monitoring of wind speed and air volume in the tunnels of the coal mine in question (previously Wuhushan Coal Mine) predominantly relies on manual wind measurement methods and sensor - based monitoring systems. Traditional ventilation parameter monitoring equipment falls short in meeting the demands for rapid and precise

intelligent ventilation parameter measurement. This deficiency can misguide ventilation technology management and decision - making processes. Consequently, given the challenge that the accuracy of wind speed monitoring in these coal mine tunnels fails to satisfy decision - making requirements, conducting in - depth research on the distribution law of wind speed across the cross - sections of coal mine tunnels holds significant importance.

In recent years, numerous domestic scholars have conducted extensive research on the distribution law of wind speed in roadway cross - sections [5-8]. Zhang Shiling [9-10] used theoretical analysis to conclude that the wind speed distribution in roadways conforms to the variation law of turbulent flow velocity and provided its logarithmic distribution formula. Lu Guangli et al. [11] investigated the variation law of airflow in roadways under different turning angles, and constructed 12 models using numerical simulation software and conducted simulation tests under different wind speeds. The results showed that the variation law of airflow in roadways remained consistent under different wind speeds, and the position of the average wind speed point in the roadway also remained fixed. Wang Hanfeng et al. [12] utilized numerical simulation software to simulate the airflow field in roadway models under different conditions and obtained the relationship between the position of the average wind speed line and the roadway cross - section. Zhang Jingzhao et al. [13] studied the impact of different positions and sizes of obstacles in underground roadways on wind speed. They combined on - site measured basic parameters of the roadway with Fluent software to construct a roadway model that conformed to the characteristics of the mine. They investigated the influence of factors such as the distance between the obstacle placed on the floor 10 m from the upstream end and the two sides of the roadway, as well as its shape, size, and placement method, on the wind speed monitoring positions in the roadway. Jiang Xiushuang et al. [14] employed the Fluent numerical simulation method to calculate the distribution of single - point test errors of the average wind speed on roadway cross - sections with various cross - sectional shapes, cross - sectional dimensions, and support methods. So, Chinese scholars have rarely studied the influence of wind speed distribution on the position of the average wind speed line in coal mine tunnel sections, and the research methods are too single, failing to fully consider the comprehensive application of multiple experimental methods and verify the reliability of theoretical calculation models from multiple aspects. Therefore, the author adopts a combined approach of theoretical calculation and numerical simulation to determine the main controlling factors affecting the wind speed distribution in roadways, establish mathematical models for the relationship between the average wind speed line and the distance from the two sides or the roof and floor of different roadway cross - section types, and reveal the wind speed distribution law in roadways under different conditions.

## 2. Theoretical model for the position of the average wind speed line

A calculation model for the distribution law of wind speed in rectangular tunnels is constructed based on the Boussinesk theory and Prandtl turbulence theory, as shown in Figure 1. The two closed dashed lines in the figure represent the wind speed contour lines at a distance  $dy$ , which are parallel to the tunnel wall. The wind speed corresponding to any point in the figure is:

$$\mu = \sqrt{\frac{\alpha \bar{v}^2}{\rho}} \frac{1}{k} \ln y + C \quad (1)$$

Where  $\mu$  is wind speed at any point, m/s;  $\bar{v}$  is average wind speed of tunnel section, m/s;  $\rho$  is air density in the tunnel, kg/m<sup>3</sup>;  $y$  is the distance from any flow layer in the tunnel to the tunnel wall, m;  $\alpha$  is the coefficient of frictional resistance;  $k$  is mixed length coefficient;  $C$  is an integral constant.

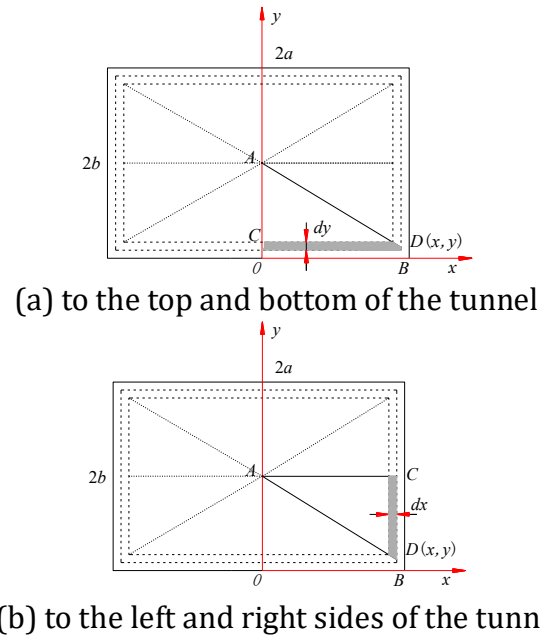


Figure 1. Calculation model for the average wind speed line position in rectangular tunnels  
According to the symmetry of the rectangular tunnel, the airflow of the entire cross-section of the rectangular tunnel  $Q$  is:

$$Q = 8 \int_0^b \left( \sqrt{\frac{\alpha v^{-2}}{\rho}} \frac{1}{k} \ln y + C \right) \left( a - \frac{a}{b} y \right) dy = 4afb \ln b - 6afb + 4abC \quad (2)$$

Where  $a$  is half of the length of the rectangular roadway;  $b$  is half the width of a rectangular roadway.

From the relationship between air volume and cross-sectional area of the tunnel, it can be concluded that the average wind speed of the rectangular section in Figure 1 (a) is:

$$\bar{v} = \frac{Q}{4ab} \quad (3)$$

Assuming that the wind speed at any point in the tunnel is the average wind speed of the tunnel, the distance from the average wind speed line of the rectangular tunnel section to the top and bottom plate after simplification is:

$$y = e^{\ln b - 1.5} \quad (4)$$

And the distance from the average wind speed line of the cross-section of the roadway to the left and right sides of the roadway can be obtained as:

$$x = e^{\ln a - 1.5} \quad (5)$$

From the expression, it can be seen that the position of the average wind speed line in a rectangular tunnel is only related to the tunnel size and is independent of other main control factors. Similarly, through theoretical derivation of the average wind speed line for rectangular tunnels with semi-circular arches, trapezoids, and circular cross-sections, consistent conclusions have been drawn. Therefore, the position of the average wind speed line in the roadway is only related to the size of the roadway and is not related to other controlling factors. In order to further discuss the influence of tunnel size on the position of the average wind speed line, common types of tunnel sizes in rectangular tunnels are listed, and the corresponding average wind speed line positions for different tunnel sizes are calculated. The influence of tunnel height and width on the position of the average wind speed line is discussed. According to the model formula, the results obtained are shown in Tables 1 and 2. According to Tables 1 and 2, it can be seen that the distance between the average wind speed line and the top and bottom (left and right sides) of the tunnel is positively correlated with the height (width) of the

tunnel. The distance between the average wind speed line and the two sides (top and bottom) of the tunnel is about 0.11 times the width (height) of the tunnel.

Table 1. Average wind speed line positions corresponding to different tunnel heights

Tunnel height (m)	2.5	3.0	3.5	4.0	4.5	5.0
Distance from top and bottom plate (m)	0.2789	0.3347	0.3905	0.4462	0.5020	0.5578
Distance from roof/height of roadway	0.11156	0.11157	0.11157	0.11155	0.11156	0.11156

Table 2. Average wind speed line positions corresponding to different tunnel widths

Tunnel width (m)	3.0	3.5	4.0	4.5	5.0	5.5
Distance from left and right sides (m)	0.3347	0.3905	0.4462	0.5020	0.5578	0.6136
Distance from left and right sides/roadway width	0.11157	0.11157	0.11155	0.11156	0.11156	0.11156

### 3. Numerical simulation of the distribution law of wind speed on the cross-section of two tunnels

Based on the actual conditions of Wuhushan Coal Mine, 2 rectangular tunnel sizes and 2 semi-circular arch tunnel sizes, 4 sets of inlet wind speeds, and 2 support types corresponding to tunnel types were selected for simulation calculations. A total of 4 models and 16 sets of simulation experiments were conducted. Establish geometric models for different cross-sectional sizes of semi-circular arches and rectangular tunnels, and provide basic simulation parameters for the two types of tunnels under different wind speeds and support methods. The length of the tunnel models is 100 meters. When modeling, the length, height, and width of the selected roadway model are in the X, Y, and Z directions. The numerical simulation geometric model is shown in Figures 2 to 3. The COMSOL Multiphysics software is used to simulate the cross-sectional wind speed of semi-circular arches and rectangular tunnels under different cross-sectional sizes, inlet wind speeds (0.8m/s, 2m/s, 4m/s, 6m/s), and different support forms (anchor spraying and anchor net). A total of 16 simulation schemes are used.

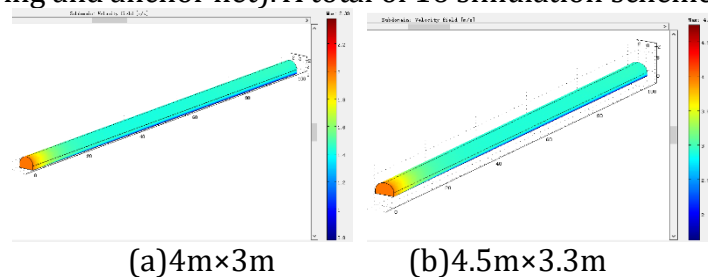
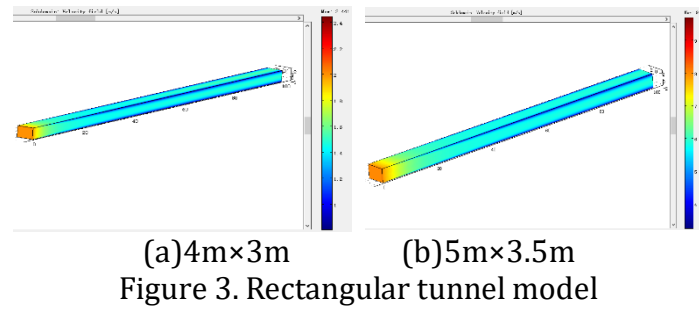


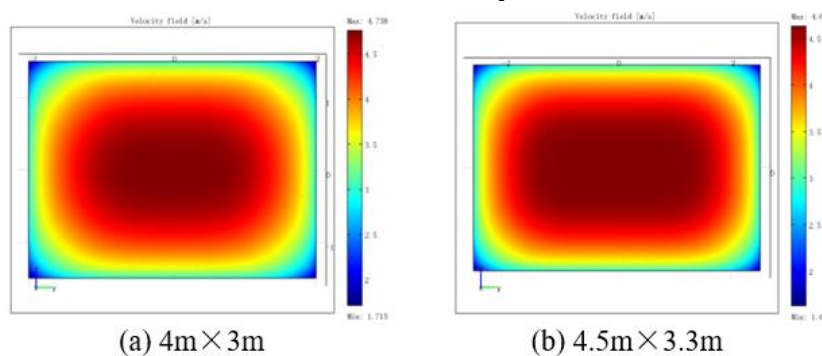
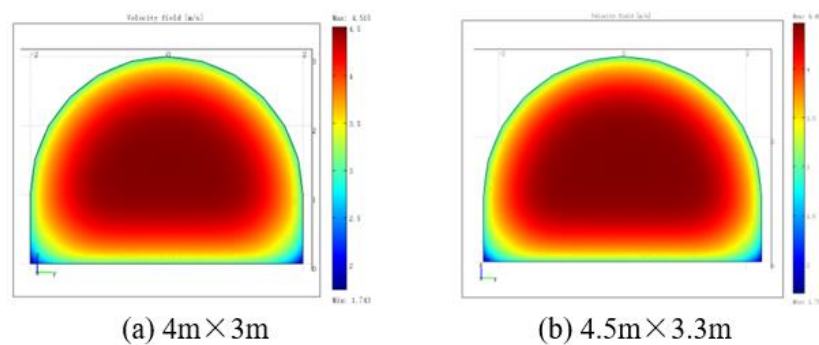
Figure 2. Semi-circular arch roadway model



#### 4. Simulation results

Distribution characteristics of wind flow field on tunnel cross-section

Contour maps with wind speeds of 4.0m/s is selected, as shown in Figures 4~5. In establishing a simplified velocity model, considering avoiding the influence of eddy currents in the tunnel flow field, a cross-sectional data at a distance of 50m from the tunnel entrance is selected as the basis. At this time, the airflow velocity field on the cross-section remains basically unchanged and reaches a fully developed state. From Figures 4 to 5, it can be seen that the contour line of the wind speed contour line on the tunnel section is consistent with the shape of the section, and the wind speed contour line is basically parallel to the tunnel wall. The wind speed contour line expands from the central part of the tunnel section to the tunnel wall. The closer the wind speed contour line is to the wall of the tunnel, the denser it is, indicating that the wind speed gradient is larger near the wall, and the sparser the wind speed contour line is closer to the middle of the tunnel, indicating that the wind speed gradient is smaller and the central wind speed of the tunnel is basically equal. In the same tunnel, the higher the average wind speed, the smaller the thickness of the near wall velocity variation layer, that is, the thickness of the boundary layer decreases with the increase of wind speed.



Distribution pattern of wind speed on the central axis

Based on the distribution of cross-sectional wind speed at  $X=50\text{m}$  in the tunnel, the inlet wind speeds are taken as  $0.8\text{m/s}$ ,  $2\text{m/s}$ ,  $4\text{m/s}$ , and  $6\text{m/s}$ , respectively. According to the selected tunnel type in the simulated scheme, an empirical formula for calculating the average wind speed of the tunnel section is obtained through the wind speed at the tunnel section point, and the relationship with the average wind speed of the tunnel is found. Using Origin 8.0 again to fit the non-linear functions of point velocity and average wind speed, the results are shown in Table 3.

Table 3. Fitting results of wind speed distribution on the central axis

Programme	Distance from the central axis to the top plate $d/\text{m}$	Inlet velocity $0.8\text{m/s}$	Inlet velocity $2\text{m/s}$	Inlet velocity $4\text{m/s}$	Inlet velocity $6\text{m/s}$
$4\text{m} \times 3\text{m}$ rectangular roadway	$d \in (0, 1.25]$	$v_{0.8} / \bar{v} = 1.1839 + 0.1633 \ln d$	$v_2 / \bar{v} = 1.1573 + 0.1391 \ln d$	$v_4 / \bar{v} = 1.1406 + 0.1267 \ln d$	$v_6 / \bar{v} = 1.1332 + 0.1189 \ln d$
	$d \in [1.25, 1.5]$	$v_{0.8} / \bar{v} = 1.225$	$v_2 / \bar{v} = 1.21$	$v_4 / \bar{v} = 1.185$	$v_6 / \bar{v} = 1.175$
$5\text{m} \times 3.5\text{m}$ rectangular roadway	$d \in [0, 1.5]$	$v_{0.8} / \bar{v} = 1.1605 + 0.1686 \ln d$	$v_2 / \bar{v} = 1.1179 + 0.1221 \ln d$	$v_4 / \bar{v} = 1.1065 + 0.1113 \ln d$	$v_6 / \bar{v} = 1.0999 + 0.1051 \ln d$
	$d \in [1.5, 1.75]$	$v_{0.8} / \bar{v} = 1.225$	$v_2 / \bar{v} = 1.175$	$v_4 / \bar{v} = 1.1575$	$v_6 / \bar{v} = 1.147$
$4\text{m} \times 3\text{m}$ semi-circular arch roadway	$d \in [0, 1.25]$	$v_{0.8} / \bar{v} = 1.173 + 0.153 \ln d$	$v_2 / \bar{v} = 1.1157 + 0.1075 \ln d$	$v_4 / \bar{v} = 1.1055 + 0.0975 \ln d$	$v_6 / \bar{v} = 1.0985 + 0.092 \ln d$
	$d \in [1.25, 1.5]$	$v_{0.8} / \bar{v} = 1.2125$	$v_2 / \bar{v} = 1.145$	$v_4 / \bar{v} = 1.1275$	$v_6 / \bar{v} = 1.118$
$4.5\text{m} \times 3.3\text{m}$ semi-circular arch roadway	$d \in [0, 1.6]$	$v_{0.8} / \bar{v} = 1.1476 + 0.1473 \ln d$	$v_2 / \bar{v} = 1.102 + 0.1038 \ln d$	$v_4 / \bar{v} = 1.0894 + 0.0908 \ln d$	$v_6 / \bar{v} = 1.0827 + 0.084 \ln d$
	$d \in [1.6, 1.65]$	$v_{0.8} / \bar{v} = 1.2$	$v_2 / \bar{v} = 1.135$	$v_4 / \bar{v} = 1.1175$	$v_6 / \bar{v} = 1.107$

### Comparison of numerical simulation and theoretical model results

There are seven indicators to analyze the relationship between wind speed and average wind speed: average wind speed, tunnel width, tunnel height, ratio of maximum wind speed to average wind speed, distance  $d$  from numerical simulation average wind speed line to roof, distance  $D$  from theoretical calculation average wind speed line to roof, and error between numerical simulation results and theoretical calculation results. Verify the reliability of the theoretical calculation model through comparative analysis. The comparison results are shown in the Table 4.

Table 4. Comparison between theoretical models and numerical simulation results

Tunnel type	Section size (Width $\times$ Height, m)	Average wind speed (m/s)	Maximum wind speed / Average wind speed	Simulated average wind speed line to roof distance $d$ (m)	Theoretical average wind speed line to roof distance $D$ (m)	Error ( $\left  \frac{d-D}{D} \right  \times 100\%$ )
Semi circular arch roadway	$4 \times 3$	0.8	1.2125	0.3228	0.3347	3.56%
		2.0	1.1450	0.3286	0.3347	1.84%



		4.0	1.1275	0.3305	0.3347	1.25%
		6.0	1.1180	0.3266	0.3347	2.42%
	4.5 × 3.3	0.8	1.2000	0.3671	0.3682	0.29%
		2.0	1.1350	0.3621	0.3682	1.66%
		4.0	1.1175	0.3628	0.3682	1.47%
		6.0	1.1070	0.3628	0.3682	1.47%
Rectangular tunnel	4 × 3	0.8	1.2250	0.3243	0.3347	3.11%
		2.0	1.2100	0.3228	0.3347	3.57%
		4.0	1.1850	0.3297	0.3347	1.51%
		6.0	1.1750	0.3262	0.3347	2.54%
	4.5 × 3.3	0.8	1.2250	0.3860	0.3905	1.16%
		2.0	1.1750	0.3808	0.3905	2.50%
		4.0	1.1575	0.3841	0.3905	1.64%
		6.0	1.1470	0.3862	0.3905	1.10%

According to Table 4, the ratio of the maximum wind speed to the average wind speed at the tunnel section is approximately 1.2. The distance between the average wind speed line of a semi-circular arch roadway and the roof is 10.76% to 1.12% of the roadway height, while the distance between the average wind speed line of a rectangular roadway and the roof is 10.76% to 11.03% of the roadway height. The error between the theoretical calculation results and the numerical simulation results is within 4%, and the conclusions of the two research methods are consistent, verifying the reliability of the theoretical model.

## 5. Conclusion

Given the pressing issue that the accuracy of wind - speed monitoring in the tunnels of Wuhushan Coal Mine falls short of meeting decision - making requirements, we adopt a synergistic approach that combines theoretical analysis with numerical simulation methods. This approach is specifically aimed at investigating the relationship between the position of the average wind - speed line and its distance from the tunnel wall. Additionally, we simulate and distill the distribution law of wind speed across the cross - sections of rectangular and semi - circular arch tunnels. The principal conclusions drawn from this study are as follows:

**(1)** We have successfully established a calculation model to determine the position of the average wind - speed line for both rectangular and semi - circular arch tunnels. Through rigorous calculations, we have derived the expressions for the average wind - speed line position for these two typical tunnel cross - sections [Insert specific expressions here if available]. The calculation results unequivocally reveal that the position of the average wind - speed line within the tunnel is solely contingent upon the tunnel's dimensions and remains unaffected by other major controlling factors. Specifically, the distance between the average wind - speed line and the two sides (top and bottom) of the tunnel is approximately 0.11 times the width (height) of the tunnel, providing a clear and quantifiable relationship.

**(2)** Our simulations show that the wind - speed contour lines within the tunnel are generally parallel to the tunnel walls, creating a distinct pattern of wind - speed distribution. A significant disparity exists in the wind - speed gradients across different regions of the tunnel. Near the

tunnel walls, the wind - speed gradient is relatively large, indicating a rapid change in wind speed over a short distance. In contrast, the wind - speed gradient in the central area of the tunnel is relatively small, suggesting a more uniform wind - speed profile. Moreover, we have observed that the thickness of the boundary layer, which is the region near the wall where the flow is affected by wall friction, decreases as the wind speed increases, highlighting the dynamic interaction between wind speed and boundary - layer characteristics.

(3) The ratio of the maximum wind speed to the average wind speed across the tunnel cross - section is approximately 1.2, providing a key metric for understanding the overall wind - speed distribution within the tunnel. Furthermore, we have determined specific position relationships between the average wind - speed line and the tunnel roof for different tunnel shapes. For a semi - circular arch roadway, the distance between the average wind - speed line and the roof ranges from 10.76% to 1.12% of the roadway height, while for a rectangular roadway, this distance varies from 10.76% to 11.03% of the roadway height. Importantly, the simulation results exhibit a high degree of accuracy, with an error margin of less than 4% when compared to the theoretical calculation results, validating the reliability of our simulation model and providing confidence in the derived conclusions.

## Acknowledgments

The study was supported by Chongqing Institute Self Reliance Project (2025YBXM37).

## References

- [1] Wang Zhixin, Liu Liren, Chen Bo, et al. Dynamic simulation of air reversal effect in coal mine ventilation system and construction of airflow regulation parameter database[J]. Industrial and Mining Automation, 2025, 51(07): 27-35.
- [2] Lu Xinming, Yin Hong. Intelligent theory and technology of mine ventilation[J]. Journal of China Coal Society, 2020, 45(06): 2236-2247.
- [3] Zhou Fubao, Wei Lianjiang, Xia Tongqiang, et al. Principle, key technologies and preliminary realization of intelligent mine ventilation[J]. Journal of China Coal Society, 2020, 45(06): 2225-2235.
- [4] Ding Cui. Numerical and experimental study on average airflow velocity distribution characteristics in trapezoidal roadways[J]. Journal of Safety Science and Technology, 2016, 12(01): 28-32.
- [5] Yang Yu, Wang Yi. Wind tunnel simulation of low-velocity airflow distribution in arched underground coal mine roadways[J]. Coal Technology, 2017, 36(06): 42-45
- [6] Hu Jianhua, Zhao Yang, Zhou Tan, et al. Multi-factor influence on airflow velocity distribution in roadway cross-sections with uneven roofs (English)[J]. Journal of Central South University, 2021, 28(07): 2067-2078.
- [7] Wang Heng, Qiu Liming, He Xueqiu, et al. Study on airflow velocity distribution in coal mine roadway cross-sections under different factors[J]. Mining Research and Development, 2022, 42(07): 125-132.
- [8] Sun Liang, Sun Zhenping. Study on airflow velocity distribution and air volume monitoring in large cross-section mine roadways[J]. Coal Technology, 2022, 41(04): 97-100.
- [9] Zhang Shiling. Study on airflow velocity measurement and variation patterns in mine ventilation roadway cross-sections[J]. Mining Safety & Environmental Protection, 2019, 46(04): 17-20.
- [10] Zhang Shiling. Underground experimental study on airflow velocity distribution characteristics in roadway cross-sections[J]. Coal Technology, 2022, 41(08): 119-122.



- [11] Lu Guangli, Wu Zanlong, Zhao Jianfeng. Numerical simulation of airflow variation patterns in roadways with different turning angles[J]. Mining Research and Development, 2019, 39(12): 116-121.
- [12] Wang Hanfeng. Simulation study on positioning monitoring of average airflow velocity points in roadway cross-sections based on Fluent[J]. Coal Science and Technology, 2015, 43(08): 92-96.
- [13] Zhang Jingzhao, Xiong Shuai, Fan Jingdao, et al. Research on the influence of roadway obstacles on airflow velocity monitoring positions[J]. Industry and Mine Automation, 2023, 49(09): 64-72.
- [14] Jiang Xiushuang, Liu Jian. Error study on single-point measurement method of average airflow velocity in roadways[J]. Journal of Safety Science and Technology, 2024, 20(08): 68-74.